Resistive Matching using an AC Boost Converter for Efficient Ultrasonic Wireless Power Transfer

Marc Bisschop
Section Bioelectronics
Delft University of Technology
Delft, The Netherlands
bisschop.mc@gmail.com

Wouter A. Serdijn
Section Bioelectronics
Delft University of Technology
Delft, The Netherlands
w.a.serdijn@tudelft.nl

***Abstract*—This paper presents a method to increase the power conversion of ultrasonic receivers in implantable medical devices. A perfect complex conjugate match between the piezo-electric receiver and the power conversion circuit is required for maximum power transfer. A boost converter in front of the rectifier enables a close to perfect resistive match. The boost converter transforms the AC voltage into a pulse width modulated square wave voltage. This saves an extra impedance transformation between the receiver and the rectifier. From circuit simulation results, it follows that this new method has the highest efficiency compared with prior art.**

***Index Terms*—impedance transformation, implantable medical devices (IMDs), maximum power transfer, resistor emulation, ultrasound, wireless power transfer.**

I. Introduction

In implantable medical devices (IMDs), there is a need for wireless power transfer as the use of batteries has several disadvantages, the biggest one being the replacement of IMDs with fully discharged batteries. Recently, interest has been growing in ultrasound (US) wireless power transfer to implants deep inside the body (>10 cm) [1]. Ultrasound has millimeter wavelength in tissue at usable frequencies (e.g., 1.6 mm at 1 MHz) [2]. The FDA allows for a time-averaged acoustic intensity of 7.2 mW/mm^2 [3] and US has low attenuation in tissue ($\sim$1 dB/MHz·cm) [1]. The impedance of an US piezo-electric receiver closely matches the power requirement of an IMD at 1-2 V [4]. These reasons enable scaling down the IMDs to millimeter sizes. Moreover, focusing of the ultrasonic waves is possible so as to ensure that the required energy will be received at the implant [5].

Little attention, however, has been paid to optimizing the electrical efficiency at the receiver and, as a consequence, much power is lost. This paper presents a design method for maximizing the usable electrical power at the IMD and proposes a new design for a close to ideal impedance match that follows from this method.

II. Ultrasonic to electrical power conversion

Piezo-electric receivers are used for converting ultrasonic waves into electric waves. Fig. 1a shows a lumped element 1D series model of an ultrasonic piezo-electric receiver around its resonance frequency in length expander mode [4]. The real part of the impedance (R_{piezo}) changes from 2.7 kΩ up to

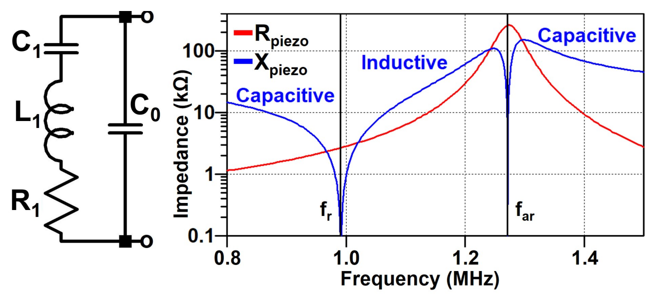

(a) (b)

Fig. 1. (a) Lumped elements 1D series model of an ultrasonic piezo-electric receiver around its resonance frequency in length expander mode. (b) impedance plot of this model for a piezo-electric element made of PZT4 and with dimensions $W = L = 1.1$ mm and $t = 1.5$ mm. Resistance R_{piezo} and reactance X_{piezo} are plotted. The capacitive and inductive regions are indicated.

260 kΩ over frequency for a square piezo-electric element made of PZT4 with equal width and length $W = L = 1.1$ mm and thickness $t = 1.5$ mm. See Fig. 1b. Between the resonance frequency ($f_r = 0.99$ MHz) and anti-resonance frequency ($f_{ar} = 1.27$ MHz) the reactance X_{piezo} is inductive. Outside this band it is capacitive [6]. The resonance frequency and anti-resonance frequency could be calculated as follows with the material properties listed in Table I [4]:

$$f_r = \frac{v}{2t} \tag{1}$$

$$f_{ar} \simeq \sqrt{1 - \frac{8k_{33}^2}{\pi^2}} f_r \tag{2}$$

The passive circuit elements of the model are calculated as [6]:

$$C_0 = \varepsilon_0 \varepsilon_{33}^T (1 - k_{33}^2) \frac{W^2}{t} \tag{3}$$

$$C_1 = \frac{8k_{33}^2 C_0}{\pi^2 - 8k_{33}^2} \tag{4}$$

$$R_1 = \frac{1}{8k_{33}^2 f_r C_0} \frac{Z_F + Z_B}{Z_C} \tag{5}$$

$$L_1 = \frac{1}{4\pi^2 f_r^2 C_1} \tag{6}$$

TABLE I
MATERIAL PROPERTIES OF A PZT4 ELEMENT [4], [6].

Sound velocity	v	4100 m/s
Acoustic impedance	Z_C	30.8 MRayls
Electrical-mechanical coupling coefficient	k_{33}	0.70
Relative permittivity	ε_{33}^T	1300
Front acoustic impedance tissue	Z_F	1.5 MRayls
Back acoustic impedance air	Z_B	400 Rayls

A perfect complex conjugate match between the impedances of the receiver and the power conversion circuit is required for maximum power transfer and preventing reflected power [7].

IMDs with wireless powering need an energy storage element due to the unreliable nature of both the received and the used power. Present IMDs, for example, are often equipped with stimulator and communication circuitry, which both consume high power for a short period of time. A rectifier is required between the piezo-electric receiver and the storage element, as electrical storage requires DC voltages. Fig. 2 shows the general block diagram of the power conversion chain of an IMD. Between all the blocks an impedance transformation should be designed to ensure optimal matching. This impedance transformation should be done both at the AC-side of the rectifier (e.g., using passive capacitors) and at the DC-side (e.g., using a boost converter).

Fig. 3 gives insight in the challenging total impedance transformation needed for maximum power transfer to the storage element. The waveform of the piezo-electric receiver voltage V_{piezo} is sinusoidal and its current I_{piezo} also, but smaller by a factor R_{piezo}. At the storage element, V_{stor} is a DC voltage. The instantaneous available electrical power is:

$$P_{el}(t) = V_{piezo}(t)I_{piezo}(t) \tag{7}$$

$$= V_{stor}(t)I_{stor}(t)\eta_{total} \tag{8}$$

where η_{total} is the total power efficiency of the power conversion system, in the ideal case equal to 1, and I_{stor} is the current into the storage element. For a constant η_{total} and a DC V_{stor}, the I_{stor} waveform is thus similar to the P_{el} waveform: a squared sinus. Consequently, the signal requires significant processing for maximum power transfer.

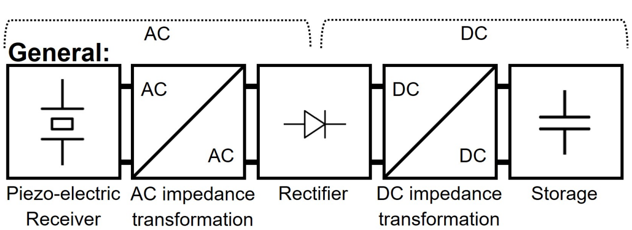

Fig. 2. General block diagram of ultrasonic wireless power transfer to an energy storage element.

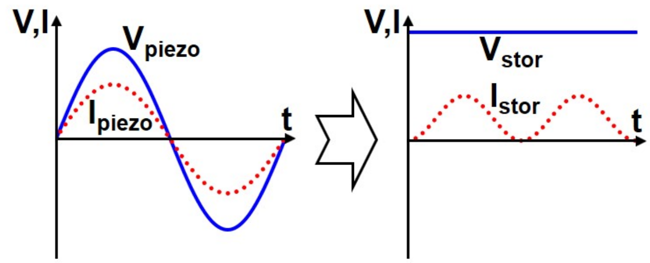

Fig. 3. V_{piezo} and I_{piezo} waveforms of a piezo-electric element operating at resonance frequency for maximum power transfer, and the V_{stor} and I_{stor} waveforms when the full P_{el} is transferred through the power conversion chain.

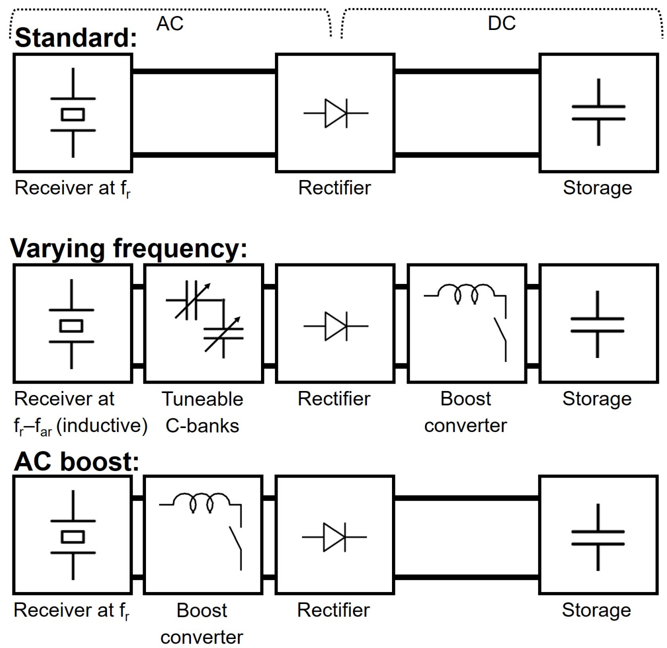

Fig. 4. Block diagrams of the three methods based on the general block diagram of Fig. 2. Standard method: without extra impedance transformations. Varying frequency method: vary across inductive band with tunable capacitor banks and DC boost converter. AC boost method: with AC boost converter operating as resistor emulation.

III. DESIGN METHODS FOR MAXIMUM POWER CONVERSION

A power conversion chain, based on the general block diagram of Fig. 2, that produces the ideal waveforms of Fig. 3 is difficult to implement as it should continuously change the matching transformation factor. However, there are methods that make it possible to design a system that produces the waveforms close to the ideal waveforms. In Fig. 4, three methods of power conversion are shown. All have a passive rectifier and a storage element so the concepts are orthogonal in itself and comparable with each other. Conventional methods are the standard method and the varying frequency method, whereas the proposed method is the AC boost method.

A. Standard: no impedance transformations

This is the basic method that is widely used, e.g., in [8]. Much of the power is lost because the current will flow only if the AC voltage V_{piezo} is larger than the voltage needed to turn on the rectifier, which is V_{stor} plus the voltage drop of the rectifier. So every cycle at least some power is lost. This solution does not efficiently handle large power fluctuations, since these induce impedance mismatches.

B. Varying frequency: vary across inductive band with tuneable capacitor bank

This method is applied in, e.g., [4]. By increasing the frequency at low acoustic power P_a, R_{piezo} increases. The peak open-circuit voltage of the piezo-electric receiver is therefore constant [8]:

$$V_{oc} = \sqrt{8 \cdot PCE \cdot P_{a,av} \cdot R_{piezo}} = \sqrt{8 \cdot P_{el,av} \cdot R_{piezo}} \quad (9)$$

where PCE is the power conversion efficiency of the piezo-electric receiver, and $P_{a,av}$ and $P_{el,av}$ are the average acoustic and electrical power, respectively.

Tuneable capacitor banks compensate for the varying inductive behaviour, which gives an increase in efficiency but has some disadvantages. Since the frequency needs to be tunable, there has to be constant communication from the IMD back to the acoustic sender about the received power, to close the control loop. This communication has a delay so the frequency and power level could only be adjusted after some cycles, resulting in a less optimal match. Further, for PZT4 material, the PCE is highest (~ 1) at f_r; at higher frequencies the PCE drops (to ~ 0.5) and the losses in tissue are higher as well.

In [4] no storage element is used. For comparability, we add a storage element to the concept and, for efficiency, a boost converter is added at the storage side of the rectifier.

C. AC boost: boosting the AC voltage

The method proposed here uses an AC boost converter at the receiver side of the rectifier. At high switching frequencies ($f_{sw} \gg f_r$), the receiver voltage V_{piezo} is boosted to a higher voltage V_{boost}, so all power can overcome the voltage barrier of the rectifier and storage element. The voltage waveform in front of the rectifier is transformed into a pulse width modulated square wave. An advantage of the boost topology is the continuous input current as is required for proper impedance matching. Another advantage is the ability to adjust the matching factor immediately, ensuring a close to ideal match.

IV. Design of AC boost: resistor emulation

To realize the maximum power transfer theorem the following relation should be implemented by the circuit when the receiver is operating at its resonance frequency:

$$I_{piezo} = V_{piezo}/R_{piezo} \quad (10)$$

where V_{piezo} is half of V_{oc} to achieve maximum power transfer. Fig. 5a shows an implementation of this concept. The current through L_{boost} (I_{piezo}) is controlled by a feedback loop with two comparators that operate the switch when it crosses the threshold values. For a situation with ideal components the result is plotted in Fig. 5b, where I_{piezo} is allowed to be

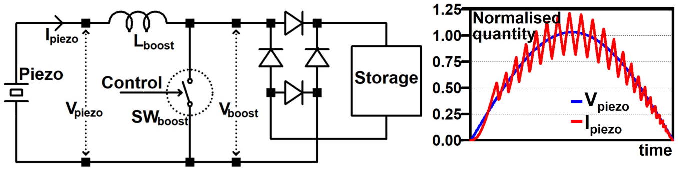

(a) (b)

Fig. 5. (a) AC Boost converter at the receiver side of the rectifier for resistor emulation. (b) Simulation of the ideal resistor emulation. The normalized V_{piezo} and I_{piezo} are plotted. The current follows the curve of the voltage so there is always a close power match.

between the threshold values of 0.8 and 1.2 times the ideal current curve. The current follows the voltage, hence (10) is fulfilled, so a close to ideal match is continuously made, ensuring maximum power transfer.

To prove the increase in power transfer, components with realistic circuit models are used in a circuit simulation. The piezo-electric receiver is made from PZT4, has a 987 kHz resonance frequency with power conversion efficiency 1.0, is 1.5 mm thick and 1.1 mm wide and long. The maximum available electrical power is 8.71 mW. Its impedance is plotted in Fig. 1b [4]. The real inductor has an inductance of 100 μH, a typical self-resonance frequency of 13 MHz ($\sim f_{sw}$), a maximum DC resistance of 12.25 Ω and a volume of 2.3 mm^3 (Coilcraft XFL2006-104ME). Two NMOS transistors, composed of 3 parallel 500 nm $\times$ 20 μm devices, operating as a bidirectional switch are designed in a standard 500 nm technology, with the technology parameters from [9]. The sizes of the switches are a trade-off between the on-resistance and the gate capacitance. The power needed to operate the switches is assumed to be lost. The voltages in the circuit are all in the allowed range of the 500 nm technology. No blocking diode is needed in the boost converter because the rectifier blocks reverse currents. The rectifier is a schottky RF rectifier (Avago HSMS282X). We assume a capacitor as the storage element, which is charged to 2 V as this is well above the transistor threshold voltage and within the specifications of current IMDs and IC technology. The same piezo-electric receiver and rectifier are also used in [4], enabling a comparison of power efficiency.

V. Efficiency comparison of the three concepts

The three methods are simulated with the components of the previous section. The standard method is simulated without a boost converter. For the varying frequency method the components at the AC-side, i.e. the piezo-electric element, the tuneable capacitor bank and the rectifier, are not simulated but the efficiency results are taken from [4]. These efficiency results are multiplied with the boost converter efficiency for every power level. An ideal blocking diode is added to the boost converter in the varying frequency method because no rectifier follows the boost converter. The extra losses of the continuous communication for frequency adjustment and control of the capacitor banks in the varying frequency method are not taken into account and zero communication delay

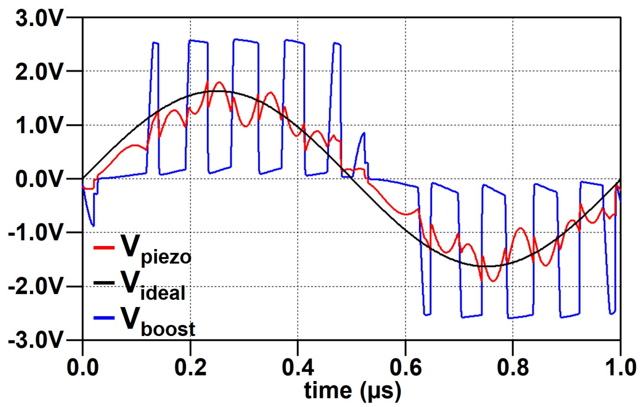

Fig. 6. Simulation results of the AC boost method for $P_{el,av} = 0.5$ mW. Plotted are the ideal V_{piezo} together with the simulated V_{piezo}. The AC boost voltage is also plotted.

is assumed so a match is made without delay. The allowed current range thresholds are optimized for maximum power transfer for both the varying frequency method and the AC boost method.

The voltage waveforms in the AC boost method are plotted in Fig. 6 for $P_{el,av} = 0.5$ mW. V_{piezo} is always close to the ideal sinusoidal voltage waveform here, providing nearly maximum power delivery by the piezo-electric receiver. The AC voltage is boosted high enough to overcome the voltage barrier of the rectifier and storage element. Sometimes the voltage is not boosted high enough because not enough energy is stored in the inductor at that moment. The control, however, does operate the switch since it does not estimate the energy stored in the inductor.

Fig. 7 shows the simulation results of the power efficiency of the three methods. The AC boost method is for the full power range the most efficient method, around $P_{load} = 1$ mW the efficiency is 74% and this drops to 22% at $P_{load} = 0.01$ mW. At $P_{load} = 2$ mW the standard method is also 74% efficient but for different power levels the efficiency is much lower, at $P_{load} = 0.1$ mW the efficiency has already dropped to 23%. The varying frequency method is as efficient as the AC boost method from $P_{load} = 0.01$ mW to $P_{load} = 0.1$ mW, but for higher power levels the efficiency is lower than the AC boost method.

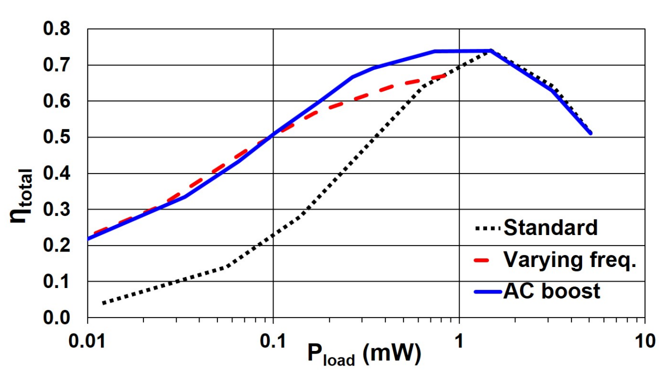

Fig. 7. Simulation results of the power efficiency as a function of load power for the three methods.

VI. Discussion and conclusions

In this paper it has been shown that, for maximum power transfer in ultrasonic wireless powering of IMDs, the impedance of the receiver has to be complex conjugate matched to the power conversion circuit. For this, two impedance transformations are needed, one at the receiver side of the rectifier and one at the storage side of the rectifier. The standard method without added impedance transformations is the least efficient as expected. The varying frequency method with tunable capacitor banks, as proposed in [4], is more efficient but has some drawbacks: fully tunable capacitor banks are required, continuous communication is needed, which has a delay and consumes power, and extra losses occur both in the tissue and the receiver. The AC boost method with a boost converter at the AC-side, as proposed here, enables resistive impedance matching over a wide output power range and has the highest power efficiency. It requires only one impedance transformation, viz. the boost converter.

The proposed method can be further improved by making a full IC design of this concept. The rectifier could be made of active components and synchronized with the boost switch. The control could also be improved by implementing an energy estimation so that the switch only closes when the inductor has enough energy to overcome the rectifier turn-on voltage and charge the storage element.

References

[1] A. Denisov and E. Yeatman, "Ultrasonic vs. inductive power delivery for miniature biomedical implants," in *Body Sensor Networks (BSN), 2010 International Conference on*. IEEE, 2010, pp. 84–89.

[2] C. R. Hill, J. C. Bamber, and G. R. ter Haar, *Physical principles of medical ultrasonics*, 2nd ed. John Wiley & Sons, Ltd, 2004.

[3] U.S. Food and Drug Administration, "Information for manufacturers seeking marketing clearance of diagnostic ultrasound systems and transducers," *Rockville, MD, USA: Center for Devices and Radiological Health*, 2008.

[4] T. C. Chang, M. J. Weber, M. L. Wang, J. Charthad, B. P. T. Khuri-Yakub, and A. Arbabian, "Design of tunable ultrasonic receivers for efficient powering of implantable medical devices with reconfigurable power loads," *IEEE transactions on ultrasonics, ferroelectrics, and frequency control*, vol. 63, no. 10, pp. 1554–1562, 2016.

[5] F. Mazzilli, C. Lafon, and C. Dehollain, "A 10.5 cm ultrasound link for deep implanted medical devices," *IEEE transactions on biomedical circuits and systems*, vol. 8, no. 5, pp. 738–750, 2014.

[6] G. S. Kino, *Acoustic waves: devices, imaging, and analog signal processing - Prentice-Hall Signal Processing Series*. Englewood Cliffs, Prentice-Hall, 1987.

[7] M. Stoopman, Y. Liu, H. J. Visser, K. Philips, and W. A. Serdijn, "Codesign of electrically short antenna–electronics interfaces in the receiving mode," *IEEE Transactions on Circuits and Systems II: Express Briefs*, vol. 62, no. 7, pp. 711–715, 2015.

[8] M. J. Weber, A. Bhat, T. C. Chang, J. Charthad, and A. Arbabian, "A miniaturized ultrasonically powered programmable optogenetic implant stimulator system," in *2016 IEEE Top. Conf. Biomed. Wirel. Technol. Networks, Sens. Syst*, 2016, pp. 12–14.

[9] B. Razavi, *Design of analog CMOS integrated circuits*, 2nd ed. McGraw-Hill Education, 2017.